ELSEVIER

Journal of Molecular Structure 328 (1994) 55–75

Journal of
MOLECULAR
STRUCTURE

Raman and infrared spectra, conformational stability, barriers to internal rotation, and ab initio calculations of trifluoroacetyl isocyanate

J.R. Durig[a,*], G.A. Guirgis[b,1], K.A. Krutules[b,2]

[a]*Department of Chemistry, University of Missouri — Kansas City, Kansas City, MO 64110-2499, USA*
[b]*Department of Chemistry and Biochemistry, University of South Carolina, Columbia, SC 29208, USA*

Received 16 May 1994

Abstract

The Raman (2500 to $10\,\mathrm{cm^{-1}}$) and infrared (2500 to $30\,\mathrm{cm^{-1}}$) spectra of trifluoroacetyl isocyanate, $CF_3C(O)NCO$, have been recorded for the gas and solid. Additionally, the Raman spectrum of the liquid has been recorded and qualitative depolarization values obtained. The observed bands are assigned on the basis of a more stable cis conformer (isocyanate group cis to the carbonyl bond) and the less stable trans conformer in the fluid phases and only the cis rotamer is present in the solid. From the variable-temperature studies of the infrared spectrum of the sample dissolved in liquified krypton, the conformer pair at 1796 and $1781\,\mathrm{cm^{-1}}$ has been used to determine the ΔH value of $163 \pm 12\,\mathrm{cm^{-1}}$ ($466 \pm 34\,\mathrm{cal\,mol^{-1}}$) which should represent closely the value of ΔH for the gas. The potential function governing conformational interchange has been determined from the asymmetric torsional frequencies and ΔH value. The values of the potential constants are: $V_1 = 356 \pm 14$, $V_2 = 1865 \pm 60$, and $V_3 = -203 \pm 6\,\mathrm{cm^{-1}}$. Additionally, variable-temperature studies of the Raman spectrum of the liquid give a ΔH of $236 \pm 30\,\mathrm{cm^{-1}}$ ($675 \pm 86\,\mathrm{cal\,mol^{-1}}$). A complete vibrational assignment is proposed for the cis conformer based on infrared band contours, Raman depolarization data, group frequencies, relative intensities, and normal coordinate calculations. Also, several of the fundamentals of the trans conformer have been assigned. The experimental conformational stability, barriers to internal rotation, structural parameters, and fundamental vibrational frequencies are compared with those obtained from ab initio gradient calculations employing the RHF/3-21G, RHF/6-31G* and/or MP2/6-31G* basis sets and to the corresponding quantities obtained for some similar molecules.

---

1. Introduction

Recently, we reported [1] the vibrational spectrum of acetyl isocyanate, $CH_3C(O)NCO$, and experimentally determined that the cis conformer (isocyanate group cis to the carbonyl bond) is more stable than the trans conformer by $449 \pm 108\,\mathrm{cm^{-1}}$ ($1.28 \pm 0.31\,\mathrm{kcal\,mol^{-1}}$) for the vapor. This result is consistent with both the microwave [2] and electron

---

[*] Corresponding author.

[1] Permanent address: Analytical R/D Department, Organic Products Division, Miles, Inc., Bushy Park Plant, Charleston SC 29411, USA.

[2] Taken in part from the thesis of K.A. Krutules which will be submitted to the Department of Chemistry and Biochemistry in partial fulfillment of the Ph.D. degree.

0022-2860/94/$07.00
SSDI 0022-2860(94)08362-L

diffraction [3] data where the investigators of both studies concluded that the cis conformer is the more stable form at ambient temperature in the gaseous state. However, it was determined from our vibrational study [1] that the conformational stability of acetyl isocyanate changes from the gas phase, where the cis conformer is more stable, to the liquid phase, where the trans conformer is more stable, by $370 \pm 60\,\mathrm{cm}^{-1}$ ($1.06 \pm 0.17\,\mathrm{kcal\,mol}^{-1}$). In the crystalline solid only the trans conformer remains.

For chlorocarbonyl isocyanate, ClC(O)NCO, most ab initio calculations [4–8] predict the cis conformer to be more stable than the trans form. However, from the vibrational study [4] of ClC(O)NCO it was determined that the trans conformer was more stable by $254 \pm 48\,\mathrm{cm}^{-1}$ ($726 \pm 137\,\mathrm{cal\,mol}^{-1}$) in the vapor state. Similarly, the trans rotamer is the stable form in the liquid and is the only conformer present in the annealed solid. The vibrational results are consistent with the electron diffraction results [5] where it was also concluded that the trans conformer is the more stable form. However, with a large basis set with electron correlation, MP2/6-311+G**, the trans conformer is predicted [6] to be more stable than the cis conformer by $871\,\mathrm{cm}^{-1}$ ($2.49\,\mathrm{kcal\,mol}^{-1}$), but the energy difference is now in error by about the same amount in the other direction.

We have also recently completed the vibrational study of fluorocarbonyl isocyanate [9], where the cis conformer has been determined to be more stable than the trans conformer in the fluid states. Similarly, ab initio calculations also predicted the cis conformer to be more stable than the trans form. From the temperature study of the infrared spectrum of the sample dissolved in liquified krypton, it has been determined that the cis conformer is more stable than the trans conformer by $150 \pm 29\,\mathrm{cm}^{-1}$ ($429 \pm 80\,\mathrm{cal\,mol}^{-1}$). The results from the vibrational study are in agreement with those from the electron diffraction [10] investigation where the cis conformer was found to be more stable than the trans form. However, it should be noted that the trans conformer is the stable form in the solid.

Thus, since the conformer stability may change from one physical state to another for these molecules, which have more than one conformer present at ambient temperature, it is difficult to predict which conformer may be the more stable form. Therefore, as a continuation of our conformational stability studies of organoisocyanates [11–19], the infrared and Raman spectra of $CF_3C(O)NCO$ have been investigated. Additionally, ab initio calculations have been carried out for comparison with the results obtained from the spectroscopic investigation.

2. Experimental

Trifluoroacetyl isocyanate was prepared by reaction of trifluoroacetyl chloride with silver cyanate. Purification was carried out using a low-temperature, low-pressure fractionation column. The pure sample was then stored at about −5°C under vacuum in a sample tube with a greaseless stopcock. All sample transfers were carried out under vacuum.

The Raman spectra were recorded on a Cary model 82 spectrophotometer equipped with a Spectra-Physics model 171 argon ion laser operating on the 5145 Å line. The spectrum of the gas was recorded using a standard Cary multipass accessory. The spectrum of the liquid was recorded from the sample contained in a Pyrex capillary. The variable-temperature study of the liquid was conducted by cooling the capillary with chilled nitrogen gas passed through a Miller–Harney cell [20]. The spectrum of the annealed solid was recorded by depositing the sample on a blackened brass block which was maintained in a cell fitted with quartz windows and cooled by boiling liquid nitrogen. Typical spectra are shown in Fig. 1, and the reported wavenumbers should be accurate to $\pm 2\,\mathrm{cm}^{-1}$ for sharp bands.

The mid-infrared spectra of the gas and annealed solid (Fig. 2) were obtained using a Digilab FTS-14C Fourier transform interferometer equipped with a Ge/KBr beamsplitter and a TGS detector. A 10 cm cell equipped with CsI windows was used to obtain the spectrum of the gas, and a KBr plate cooled with liquid nitrogen was used as the sample substrate for the spectrum of the solid. The spectrum of the annealed solid at a resolution of $1\,\mathrm{cm}^{-1}$ was obtained after several cycles of warming and cooling of the sample.

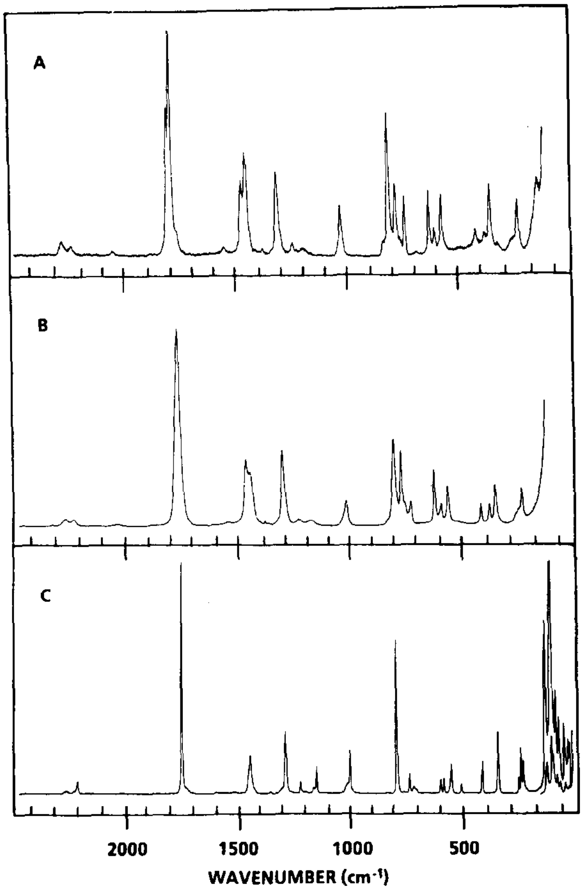

Fig. 1. Raman spectra of trifluoroacetyl isocyanate: (A) gas; (B) liquid; (C) annealed solid.

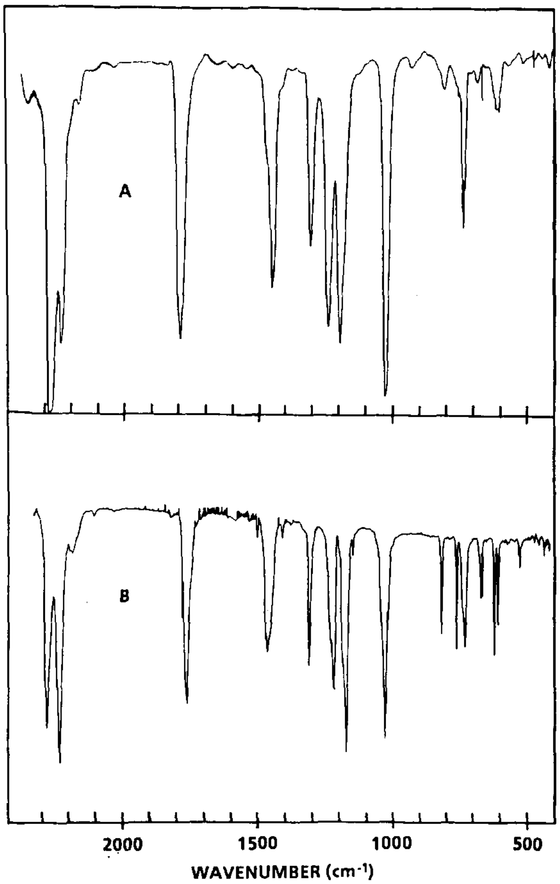

Fig. 2. Mid-infrared spectra of trifluoroacetyl isocyanate: (A) gas; (B) annealed solid.

The FT-Raman spectrum of $CF_3C(O)NCO$ was recorded on a Bruker model IFS 66 interferometer equipped with a model FRA 106 FT-Raman attachment. The spectrum was obtained utilizing a Nd:YAG laser operating on the 1.064 μm line and a liquid nitrogen-cooled Ge detector. The spectrum of the liquid was recorded from the sample contained in a Pyrex capillary. The sample was placed directly into the sample holder of the Raman attachment and the data were recorded by co-addition of 500 scans at 4.0 cm^{-1} resolution.

The mid-infrared spectra of the sample dissolved in liquified krypton as a function of temperature were recorded on a Bruker model IFS 66 Fourier transform interferometer equipped with a Globar source, Ge/KBr beamsplitter, and a TGS detector. In all cases, 200 interferograms were collected at 0.5 cm^{-1} resolution, averaged and transformed with a boxcar truncation function.

For the studies in the liquified noble gas, a specially designed cryostat cell was used which consists of a copper cell with a pathlength of 4 cm with wedged silicon windows sealed to the cell with indium gaskets. It is cooled by boiling liquid nitrogen, and the temperature is monitored with two Pt thermoresistors. The complete cell is connected to a pressure manifold to allow for the filling and evacuation of the cell. After the cell is cooled to the desired temperature, a small amount of the compound is condensed into the cell. Next, the pressure manifold and the cell are pressurized with the noble gas, which immediately starts condensing in the cell, allowing the compound to dissolve.

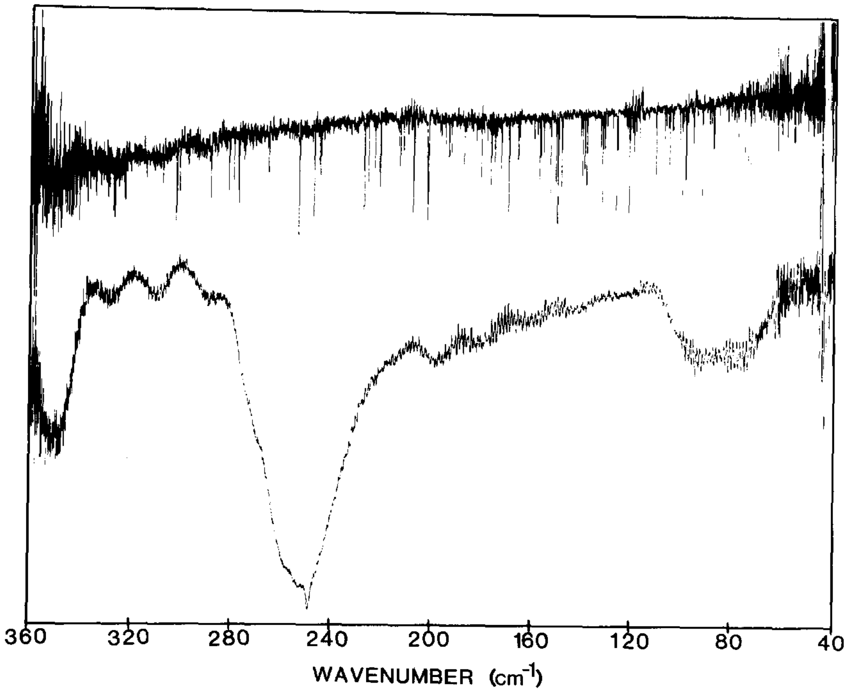

Fig. 3. Far-infrared spectrum of trifluoroacetyl isocyanate, with the top spectrum that of water.

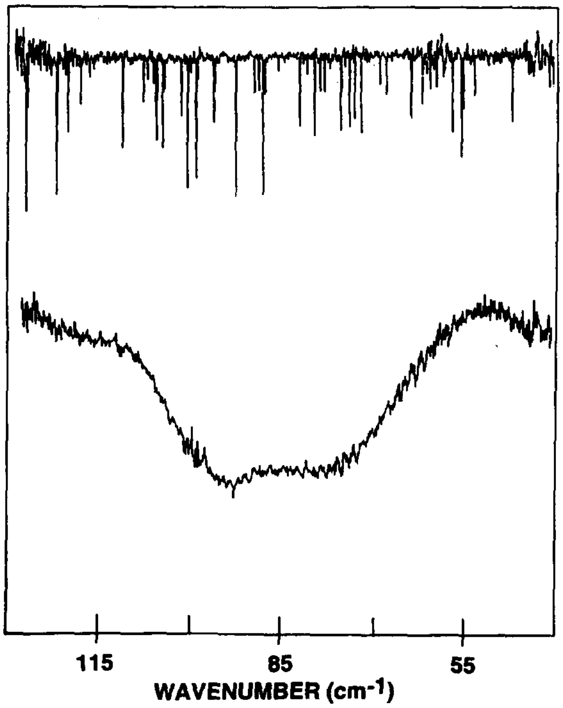

Fig. 4. Far-infrared spectrum of gaseous trifluoroacetyl isocyanate in the region of the asymmetric torsion, with the top spectrum that of water.

The far-infrared spectrum from which the torsional transitions were measured (Figs. 3 and 4) was recorded on a Bomem model DA3.002 Fourier transform interferometer equipped with a vacuum bench, a Globar source, and a liquid helium-cooled silicon bolometer with a wedged sapphire filter and polyethylene windows. The gaseous sample was contained in a 1 m cell equipped with polyethylene windows and recorded at a spectral resolution of 0.1 cm^{-1} with 6.25 and 25 μm Mylar beamsplitters. Typically, 256 scans were needed to give a satisfactory signal-to-noise ratio. All of the observed infrared and Raman bands are listed in Table 1.

3. Conformational analysis

The Raman spectra of the gas and liquid clearly show the presence of both the cis and trans conformers, whereas only one conformer exists in the solid. A number of bands disappear with crystallization. These bands occur at 380, 626, 776, and 1443 cm^{-1} and one of the carbonyl stretches at either 1796 or 1781 cm^{-1}. These data clearly show the presence of two conformers in the fluid states with only one form remaining in the solid. However, there appears to be some conflicting data, making it difficult to determine the conformational stability and to determine which conformer remains in the solid.

Since the assignment of the fundamental vibrations is not straightforward and it is not clear which conformer remains in the solid, ab initio calculated frequencies were obtained with both the MP2/6-31G* and RHF/6-31G* basis sets. The predicted frequencies of both conformers were then compared with the experimental frequencies in an attempt to determine which conformer disappears with crystallization. The band which is observed at 808 cm^{-1} in the Raman spectrum of the gas and remains in the Raman spectrum of the solid is assigned to the C–N stretch. This frequency corresponds better to the unscaled frequency of 821 cm^{-1} obtained with the MP2/6-31G* basis set for the cis conformer than the frequency of 779 cm^{-1} obtained with the same basis set for the C–N stretch of the trans conformer. This predicted frequency of 779 cm^{-1} for the C–N stretch of the trans conformer corresponds well with the observed band at 776 cm^{-1} in the Raman spectrum of the gas which disappears from the spectrum of the solid. Additionally, the observed band at 737 cm^{-1} in the Raman spectrum of the gas which also remains in the spectrum of the solid agrees well with the unscaled frequency of 729 cm^{-1} for the CF_3 symmetric deformation (MP2/6-31G* basis set) predicted for the cis conformer. Similarly, the observed band at 601 cm^{-1} in the Raman spectrum of the gas which remains in the spectrum of the solid agrees better with the frequency of 597 cm^{-1} predicted for the cis conformer than with the calculated frequency of 619 cm^{-1} for the trans rotamer. The band at 354 cm^{-1} in the Raman spectrum of the solid also corresponds better with the frequency of 351 cm^{-1}, which is the frequency predicted for the cis conformer compared to 380 cm^{-1} predicted for the trans form. Therefore, from considering the low-frequency bands from 900 to 200 cm^{-1} which remain in the spectra of the solid, it appears that the cis conformer is the rotamer present in this physical state.

Variable-temperature studies of the Raman spectra of the gas and liquid were conducted to determine the more stable conformer in the fluid phases. The conformer pair at 808 and 776 cm^{-1} which is assigned to the C–N stretch of the cis and trans conformers, respectively, were used to determine the more stable conformer in the fluid states. The band at 776 cm^{-1} increases in intensity as the temperature is increased (Table 2) for both the gas and liquid. Thus, the trans rotamer is less stable than the cis conformer in the fluid states.

There are two bands at 1796 and 1781 cm^{-1} in the Raman spectrum of the gas that appear in the carbonyl stretching region. With the MP2/6-31G* basis set, the frequency predicted for the CO stretch for the cis conformer is slightly lower than that for the trans conformer. However, since a shift in frequency from the gas to solid is characteristic of the carbonyl stretch, it is difficult to predict which band disappears with crystallization. Therefore, variable-temperature studies of the sample dissolved in liquified krypton (Fig. 5) were carried out and the band at 1781 cm^{-1}, which is assigned to the cis conformer, is indeed found to be the CO stretch of the more stable conformer.

A problem arises with the assignment of the two bands in the NCO symmetric stretching region. There are two bands at 1463 and 1443 cm^{-1} in the Raman spectrum of the gas, with the latter band disappearing with crystallization. In the infrared spectrum of the gas there is a strong band at 1442 cm^{-1} with a shoulder at 1462 cm^{-1}, and in the infrared spectrum of the solid, a sharp band at 1459 cm^{-1}. Using RHF/6-31G* scaled frequencies, the NCO symmetric stretch of the cis conformer is predicted to be about 50 cm^{-1} lower in frequency than that predicted for the trans conformer. However, with the MP2/6-31G* basis set, the NCO symmetric stretch of the cis conformer is predicted at approximately the same frequency for the corresponding mode of the trans conformer, i.e. 1502 and 1498 cm^{-1}, respectively. Thus, it is difficult to make a reliable assignment for the NCO symmetric stretch for the two rotamers based on the calculated frequencies. Variable-temperature studies of the infrared spectrum of the sample dissolved in liquified krypton and of the Raman spectrum of the gas were conducted. The results from the latter study were inconclusive. From the

Table 1
Observed[a] infrared and Raman frequencies (cm^{-1}) for trifluoroacetyl isocyanate

Infrared				Raman						Assignment	
Gas	Rel. int.	Solid	Rel. int.	Gas	Rel. int.	Liquid	Rel. int. and depol.	Solid	Rel. int.	ν_i[b]	Approximate description
								2291	sh		
2275 max	vs	2281	s	2277	w	2273	5.2	280	vw		$\nu_5 + \nu_6$
2235 max	s	2232	vs	2235	w	2235	w	2232	w	ν_1	NCO antisymmetric stretch
2173	w	2193	m								
1795 max	sh			1796	m					ν_2'	CO stretch
		1779	m								
1785 max	s	1760	s	1781	s	1768	100.0,p	1771	s	ν_2	CO stretch
1777 max	sh										
				1543	w	1545	w				$\nu_7 + \nu_8$
		1500	w								
1462	sh	1460	m	1463	m	1466	35.0,p	1463	m	ν_3	NCO symmetric stretch
1442 max	s			1443	m	1447	29.5,p			ν_3'	NCO symmetric stretch
1402	sh	1403	w								$\nu_7 + \nu_9$
				1336	vw	1330	sh	1324	vw		$\nu_5 + \nu_{14}$
1303 max	m	1301	s	1309	m	1304	31.3,p	1304	m	ν_4	CC stretch
1243		1222	sh								
1235 max	s	1211	s	1240	w,bd	1234	w	1237	w	ν_5	CF_3 antisymmetric stretch
1195 *R*		1176	sh								
1192 *Q*	s	1167	s	1195	w	1180	w,	1180	w	ν_{15}	CF_3 antisymmetric stretch
		1164	s								
1120	w	1138	w								
1027 *R*		1027	sh					1035	w		
1025 ctr,*B*	s	1018	s	1025	m	1020	11.6,p	1019	m	ν_6	CF_3 symmetric stretch
1023 *P*		1014	s								
1019	sh										
928	w										
830	vw			834	w	837	vw				$\nu_8 + \nu_{14}$
807 max	w	806	s	808	m	808	51.0,p	809	s	ν_7	CN stretch
				776	m	776	41.9,p			ν_7'	CN stretch
752 max	w	750	s	755	vw,bd	760	vw	752	w	ν_{16}	CC(O)N bend
738 *R*											
734 *Q*,*A*	m	727	sh	737	m	735	15.1,p	734	w	ν_8	CF_3 symmetric deformation
730 *P*		720	s								
		663		687	w,bd						
		659									
		654									
				626	m	629	27.7,p		w	ν_8'	CF_3 symmetric deformation
618 *Q*											
611		611									
604 *Q*		597	s							ν_{17}	NCO bend
								613			
				601	w	600	10.9,p	598	w	ν_9	NCO bend
570 max	w	572	w	571	m	569	21.3,p	565	w	ν_{10}	CF_3 antisymmetric deformation

Table 1 (continued)

Infrared				Raman						Assignment	
Gas	Rel. int.	Solid	Rel. int.	Gas	Rel. int.	Liquid	Rel. int. and depol.	Solid	Rel. int.	ν_i^b	Approximate description
517 max	w	519	w			525	vw,dp	520	w	ν_{18}	CF_3 antisymmetric deformation
444 max	w										
								428	sh		
418 max	w			420	w	421	14.3,p	425	w	ν_{11}	CC(O)N bend
				380	w	382	14.2,p			ν'_{11}	CC(O)N bend
				355	m	356	25.9,p	354	m	ν_{12}	CF_3 rock
								261	w		
				254	sh,bd	251	w,bd,dp	250	m	ν_{19}	CF_3 rock
				232	m	236	19.3,p	240	m	ν_{13}	CCN deformation
				140	w			137			$2\nu_{20}$
								115			
93	vw									ν'_{20}	NCO torsion (1 ← 0)
90	vw			90	vw			92		ν_{14}	CNC bend
75	vw							79		ν_{20}	NCO torsion (1 ← 0)
								57			
								39			

[a] Abbreviations used; s, strong; m, medium; v,very; w, weak; sh, shoulder; p, polarized; dp, depolarized; bd, broad; min, minimum; ctr, center; *P*, *Q*, and *R* refer to vibrational–rotational infrared band contours.

[b] ν' denotes fundamental arising from the trans conformer.

infrared study, it appears that the band at 1442 cm^{-1} is a fundamental vibration of the more stable conformer. However, there is an interfering band at 1436 cm^{-1}, making it difficult to obtain a reliable result. Therefore, since all other data suggest that the cis conformer is more stable than the trans form in the fluid states, and this conformer is the only form remaining in the solid, the NCO symmetric stretch of the cis conformer is assigned to the band at 1463 cm^{-1} in the Raman and infrared spectra of the gas.

Table 2
Temperature and intensity ratios for the conformational study of gaseous and liquid trifluoroacetyl isocyanate

	T (°C)	$10^3/T$ (K^{-1})	$K = I_t/I_c$	$-\ln K$
Krypton	−106	5.99	0.421	0.866
	−114	6.29	0.373	0.985
	−122	6.62	0.339	1.082
	−130	6.99	0.324	1.126
	−138	7.41	0.295	1.221
	−146	7.87	0.263	1.366
Liquid	22	3.39	0.829	0.188
	9	3.54	0.754	0.282
	−8	3.77	0.692	0.368
	−21	3.97	0.639	0.449
	−39	4.27	0.575	0.553
	−54	4.56	0.548	0.602
	−69	4.90	0.484	0.725

To obtain the experimental ΔH of $CF_3C(O)NCO$, variable-temperature studies of the infrared spectrum of the sample dissolved in liquified krypton were conducted. An important advantage of this type of temperature study is that conformer peaks are better resolved and the areas under them more easily measured than bands observed in the infrared spectrum of the gas. For example, two well-resolved bands are observed in the CO stretching region in the infrared spectrum of the liquified noble gas solution (Fig. 5) compared with only one band being observed in this spectral region in the infrared spectrum of the gas (Fig. 2). The conformer pair at 1796/1781 cm^{-1} were used experimentally to determine the ΔH value. The mid-infrared spectra of the liquified noble gas solution

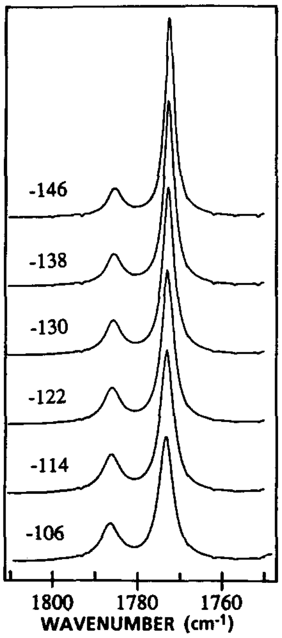

Fig. 5. Temperature dependence (in °C) of the mid-infrared spectrum of trifluoroacetyl isocyanate dissolved in liquified krypton for the conformer pair at 1796 (trans) and 1781 (cis) cm^{-1}.

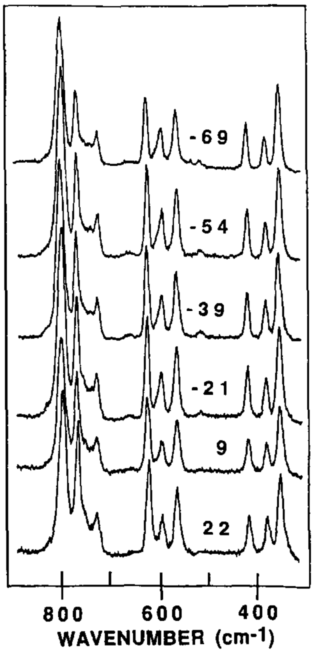

Fig. 7. Temperature dependence (in °C) of the Raman spectra of the liquid phase from 900 to 300 cm^{-1}.

were recorded at six different temperatures ranging from 127 to 167 K (Table 2). By using the van't Hoff isochore, $-\ln K = (\Delta H/RT) - \Delta S/R$, the enthalpy difference between the cis and trans conformers can be calculated. A plot of $-\ln K$ versus $1/T$, where K is the ratio of the intensity of a band resulting from the trans conformer to one resulting from the cis conformer, has a slope which is proportional to the enthalpy difference. The results are given in Table 2 and graphically displayed in Fig. 6 yield a value of ΔH of $163 \pm 12\,cm^{-1}$ ($466 \pm 34\,cal\,mol^{-1}$). It is clear that the 1781 cm^{-1} band assigned to the CO stretch of the cis conformer increases in intensity as the temperature is decreased and thus is the stable conformer in the gas.

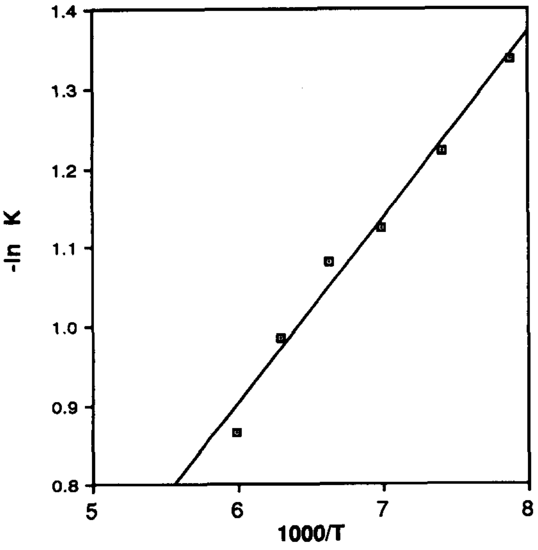

Fig. 6. Plot of $-\ln(I_{1796}/I_{1781})$ versus $1000/T$. The slope of the best-fit line is 235.

To obtain more information on the conformational stability of trifluoroacetyl isocyanate, a variable-temperature study of the Raman spectrum of the liquid was conducted. Measurements were made at seven different temperatures ranging from −69 to 22°C for the region from 900 to 300 cm^{-1} (Fig. 7). Based on the slope of the best-fit line, the bands at 776/808 cm^{-1} were used to determine a value of $236 \pm 30\,cm^{-1}$ ($675 \pm 86\,cal\,mol^{-1}$). From the spectral data, the decrease in the intensity of the Raman lines assigned to the trans conformer as the temperature decreases indicates that the trans conformer is less stable than the cis conformer in the liquid.

Additionally, the gas-phase enthalpy difference was calculated using the relative intensities and the calculated Raman activities of the following conformer pairs: 1796/1781, 1443/1463, 776/808, and 629/737 cm^{-1}. This procedure gave a ΔH value of 164 ± 52 cm^{-1} (469 ± 149 cal mol^{-1}), which is in excellent agreement with the experimental value of 163 ± 12 cm^{-1} obtained from the variable temperature studies of the liquified krypton solution.

4. Vibrational assignment

The cis and trans conformers of trifluoroacetyl isocyanate have C_s symmetry and should exhibit 21 fundamental vibrations spanning the irreducible representations 14 A′ and 7 A″. The A′ vibrations are expected to give rise to *A*, *B* and *A*/*B* hybrid infrared gas-phase band contours and polarized Raman lines. The A″ vibrations are expected to exhibit *C*-type infrared band contours and depolarized Raman lines. Assignments are based on infrared band contours, relative intensities, Raman depolarization ratios, and group frequencies, along with support from the normal coordinate calculations.

The strong band at 2235 cm^{-1} in the infrared spectrum of the gas is characteristic of the NCO antisymmetric stretch and thus is assigned to this fundamental of the cis conformer. There are two bands in the CO stretching region in the Raman spectrum of the gas and the ab initio calculations predict the CO stretch of the cis conformer to have a lower frequency than that for the trans rotamer. Thus, the lower frequency band at 1781 cm^{-1} in the Raman spectrum of the gas is assigned to the CO stretch of the cis rotamer, whereas the band at 1796 cm^{-1} is assigned to this mode for the trans conformer. There are two bands (1463 and 1443 cm^{-1}) in the Raman spectrum of the gas

Table 3
Structural parameters[a], rotational constants, and dipole moments for trifluoroacetyl isocyanate

Parameter	Cis			Trans[b]	
	RHF/3-21G	RHF/6-31G*	MP2/6-31G*	RHF/6-31G*	MP2/6-31G*
$r(C_1–N)$	1.365	1.385	1.399	1.382	1.395
$r(N=C_3)$	1.189	1.215	1.235	1.204	1.232
$r(C_3=O_4)$	1.156	1.134	1.174	1.139	1.176
$r(C_1=O_5)$	1.196	1.179	1.213	1.173	1.209
$r(C_1–C_6)$	1.511	1.531	1.531	1.535	1.537
$r(C–F_7)$	1.336	1.306	1.334	1.301	1.329
$r(C–F_{8,9})$	1.344	1.316	1.345	1.321	1.350
$\sphericalangle C–N=C$	147.4	126.5	127.8	136.2	131.9
$\sphericalangle N–C_1=O$	126.2	126.4	126.9	123.8	124.0
$\sphericalangle C–C–N$	110.3	111.4	110.2	114.7	113.8
$\sphericalangle F_7–C–C$	110.5	110.6	110.7	111.5	111.4
$\sphericalangle F_7–C_6–H_8$	109.0	108.9	109.0	109.2	109.3
$\sphericalangle F_8–C_6–H_9$	107.9	108.5	108.4	107.7	107.6
$\sphericalangle N=C=O$	175.2	174.4	172.7	174.1	172.1
A	3345	3680	3495	2758	2644
B	1013	1002	980	1376	1385
C	902	911	887	1089	1085
$\lvert\mu_a\rvert$	0.874	0.862	0.762	0.710	0.762
$\lvert\mu_b\rvert$	0.312	0.923	0.905	1.034	1.021
$\lvert\mu_c\rvert$	0.0	0.0	0.0	0.0	0.0
$\lvert\mu_t\rvert$	0.928	1.263	1.183	1.254	1.274
$-(E+612)$	0.703046	4.105718	5.525306	4.101509	5.523717

[a] Bond lengths in Ångströms, bond angles in degrees, rotational constants in MHz, dipole moments in Debyes, and energies in Hartree.
[b] For the 3-21G basis set there is no stable trans conformer.

that are in the NCO symmetric stretch region and, as indicated earlier, the higher frequency band is assigned to the cis conformer.

The three CF_3 stretches have strong characteristic bands in the infrared spectrum and the one at 1235 cm^{-1} is assigned to the A′ CF_3 antisymmetric stretch. The A″ CF_3 antisymmetric stretch is assigned to the band at 1192 cm^{-1} and the strong *B*-type band at 1025 cm^{-1} is assigned to the CF_3 symmetric stretch. This assignment is consistent with the frequency order obtained from the ab initio calculations. The assignments for the C–N stretch and CF_3 symmetric deformation for both conformers have been described earlier. The A′ CF_3 antisymmetric deformation is assigned to the band at 571 cm^{-1} and the weak band at 517 cm^{-1} to the corresponding A″ mode for the cis conformer.

The A″ CC(O)N bend is assigned to the band at 752 cm^{-1} in the infrared spectrum of the gas. The band at 420 cm^{-1} in the Raman spectrum of the gas which has a corresponding band at 425 cm^{-1} in the Raman spectrum of the solid is assigned to the A′ CC(O)N bend of the cis conformer. Thus, the band at 380 cm^{-1} in the Raman spectrum of the gas which does not have a counterpart in the solid is assigned to the A′ CC(O)N bend of the trans conformer. The A″ NCO bend is assigned to the band at 611 cm^{-1} in the infrared spectrum of the gas, whereas the A′ mode is assigned to the polarized band at 600 cm^{-1} in the Raman spectrum of the liquid.

The A′ CF_3 rock is assigned to the 355 cm^{-1} band and the corresponding A″ mode is assigned to the band at 254 cm^{-1}, whereas the band at 232 cm^{-1} is assigned to the CCN deformation. The CNC bend is assigned to the weak band at 90 cm^{-1} and the NCO torsion of the cis conformer is assigned to the band at 75 cm^{-1}. The corresponding fundamental of the trans conformer is assigned to the band at 93 cm^{-1}. These assignments are summarized in Table 1 and are supported by the normal coordinate calculations.

Table 4
Symmetry coordinates for trifluoroacetyl isocyanate

Species	Description	Symmetry coordinate[a]
A′	NCO antisymmetric stretch	$S_1 = P - T$
	CO stretch	$S_2 = R$
	NCO symmetric stretch	$S_3 = P + T$
	CC stretch	$S_4 = D$
	CF_3 antisymmetric stretch	$S_5 = 2r_1 - r_2 - r_3$
	CF_3 symmetric stretch	$S_6 = r_1 + r_2 + r_3$
	CN stretch	$S_7 = Q$
	CF_3 symmetric deformation	$S_8 = \alpha_1 + \alpha_2 + \alpha_3 - \beta_1 - \beta_2 - \beta_3$
	NCO bend	$S_9 = \mu$
	CF_3 antisymmetric deformation	$S_{10} = 2\alpha_1 - \alpha_2 - \alpha_3$
	CC(O)N bend	$S_{11} = \gamma - \epsilon$
	CF_3 rock	$S_{12} = 2\beta_1 - \beta_2 - \beta_3$
	CCN deformation	$S_{13} = 2\delta - \epsilon - \gamma$
	CNC bend	$S_{14} = \sigma$
	Redundancy	$S_{1R} = \gamma + \epsilon + \delta$
	Redundancy	$S_{2R} = \alpha_1 + \alpha_2 + \alpha_3 + \beta_1 + \beta_2 + \beta_3$
A″	CF_3 antisymmetric stretch	$S_{15} = r_2 - r_3$
	CC(O)N bend	$S_{16} = \omega$
	NCO bend	$S_{17} = \pi$
	CF_3 antisymmetric deformation	$S_{18} = \alpha_2 - \alpha_3$
	CF_3 rock	$S_{19} = \beta_2 - \beta_3$
	NCO torsion	$S_{20} = \tau_2$
	CF_3 torsion	$S_{21} = \tau_1$

[a] Not normalized.

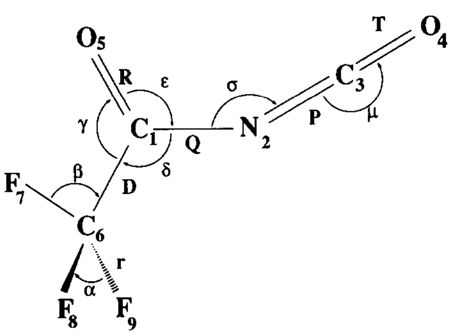

Fig. 8. Molecular diagram showing internal coordinates for the cis conformer of trifluoroacetyl isocyanate.

5. Ab initio calculations

The LCAO-MO-SCF restricted Hartree–Fock calculations were performed with the GAUSSIAN-90 program [21] with Gaussian-type basis functions. The energy minima with respect to the nuclear coordinates were obtained by the simultaneous relaxation of all the geometric parameters using the gradient method of Pulay [22]. Calculated structural parameters determined with the RHF/3-21G, RHF/6-31G* and MP2/6-31G* basis sets are given in Table 3 for the cis and trans conformations. The energy differences that resulted from the RHF/6-31G* and MP2/6-31G* basis sets are 924 $\mathrm{cm^{-1}}$ (2.6 $\mathrm{kcal\,mol^{-1}}$) and 349 $\mathrm{cm^{-1}}$ (998 $\mathrm{cal\,mol^{-1}}$), respectively, with the cis form lower in energy than the trans conformer.

For the normal coordinate analysis, the force field in Cartesian coordinates was calculated by the GAUSSIAN-90 program [21] with the MP2/6-31G* basis set. Internal coordinates were defined as shown in Fig. 8, and were used to form the symmetry coordinates listed in Table 4. The Cartesian coordinates obtained for the optimized geometry were used to calculate the ***B***-matrix elements with the *G*-matrix program of Schachtschneider [23]. These ***B***-matrix elements were used to convert the ab initio force field in Cartesian coordinates to a force field in desired internal coordinates. The resulting force fields for the cis and trans conformers are given in Tables 5 and 6, respectively. These force fields were used in a mass-weighted Cartesian coordinate calculation to reproduce the ab initio vibrational frequencies and to determine the potential energy distribution (P.E.D.) which is given in Table 7 for the two conformers. The normal coordinate analysis was repeated with the RHF/6-31G* basis set and the results are given in Table 8 for the two conformers. The diagonal elements of the force field in internal coordinates were then assigned scaling factors of 0.9 for stretching, 0.8 for bending and 1.0 for torsional coordinates and the calculation repeated to obtain the fixed scaled force field and scaled vibrational frequencies. The scaled frequencies are in better agreement with the experimentally observed frequencies than the unscaled with 5 or 6% average disagreement rather than 15% or more disagreement displayed by the unmodified ab initio results. Nevertheless, these data are not as good as the calculated wavenumbers obtained with the MP2/6-31G* basis set, but for many molecules they are sufficient to support the vibrational assignments and conformer identifications.

Raman and infrared spectra were calculated (Figs. 9 and 10) using frequencies and infrared intensities determined from the MP2/6-31G* basis set and Raman scattering activities determined from the RHF/6-31G* basis set. The Raman scattering cross-sections, $\partial\sigma_j/\partial\Omega$, which are proportional to Raman intensities, can be calculated from the scattering activities and the predicted frequencies for each normal mode using the relationship [24]:

$$\frac{\partial\sigma_j}{\partial\Omega} = \left(\frac{2^4\pi^4}{45}\right)\left(\frac{(\nu_0-\nu_j)^4}{1-\exp\left[\dfrac{-hc\nu_j}{kT}\right]}\right)\left(\frac{h}{8\pi^2c\nu_j}\right)S_j$$

where ν_0 is the exciting frequency, ν_j is the vibrational frequency of the jth normal mode, and S_j is the corresponding Raman scattering activity. To obtain the polarized Raman scattering cross-sections, the polarizabilities are incorporated into S_j by $S_j[(1-\rho_j)/(1+\rho_j)]$ where ρ_j is the depolarization ratio of the jth normal mode. The Raman scattering cross-sections and calculated frequencies were used together with a Lorentzian function to obtain the calculated spectrum. Since the calculated frequencies are approximately 10% higher than those observed, the frequency axis of the theoretical spectrum was shifted by a factor of 0.9. The predicted Raman spectra of the cis and

Table 5
Ab initio harmonic force constants (mdyn Å^{-1}) for the cis conformer of trifluoroacetyl isocyanate

	Q	P	T	R	D	r_1	r_2	r_3	γ	μ	σ	δ
Q	5.929	0.258	−0.451	1.240	0.242	0.105	0.129	0.129	−0.365	0.008	0.371	0.263
P		13.519	0.717	−0.250	−0.017	0.013	−0.018	−0.018	0.065	0.359	0.800	0.205
T			16.375	0.193	0.000	0.044	0.025	0.025	−0.042	0.047	−0.235	−0.024
R				13.279	0.446	0.033	0.070	0.070	0.158	0.042	0.092	−0.357
D					4.580	0.222	0.267	0.267	0.054	0.001	0.007	0.171
r_1						6.996	0.752	0.752	−0.123	−0.003	0.018	0.154
r_2							6.646	0.755	0.098	0.007	0.003	−0.038
r_3								6.646	0.098	0.007	0.003	−0.038
γ									0.661	−0.012	−0.030	−0.283
μ										0.695	0.034	−0.006
σ											0.377	0.021
δ												0.698
ϵ												
β_1												
β_2												
β_3												
α_1												
α_2												
α_3												
ω												
π												
τ_1												
τ_2												

Table 6
Ab initio harmonic force constants (mdyn Å^{-1}) for the trans conformer of trifluoroacetyl isocyanate

	Q	P	T	R	D	r_1	r_2	r_3	γ	μ	σ	δ
Q	6.057	0.216	−0.382	1.264	0.272	0.062	0.164	0.164	−0.407	−0.015	0.446	0.221
P		13.754	0.709	−0.037	−0.071	-0.065	−0.050	−0.050	−0.024	0.371	0.838	−0.153
T			16.243	0.085	−0.003	0.039	0.080	0.080	−0.036	0.054	−0.196	0.004
R				13.557	0.500	0.041	0.071	0.071	0.164	0.035	0.023	−0.357
D					4.371	0.203	0.277	0.277	0.045	0.004	0.077	0.207
r_1						7.142	0.736	0.736	−0.119	−0.003	−0.009	0.133
r_2							6.469	0.750	0.081	0.013	0.043	−0.013
r_3								6.469	0.081	0.013	0.043	−0.013
γ									0.685	0.003	−0.100	−0.336
μ										0.716	−0.029	0.011
σ											0.485	0.143
δ												0.772
ϵ												
β_1												
β_2												
β_3												
α_1												
α_2												
α_3												
ω												
π												
τ_1												
τ_2												

ϵ	β_1	β_2	β_3	α_1	α_2	α_3	ω	π	τ_1	τ_2
0.102	0.158	−0.004	−0.004	−0.089	−0.034	−0.034	0.000	0.000	0.000	0.000
−0.270	0.053	−0.052	−0.052	−0.007	0.029	0.029	0.000	0.000	0.000	0.000
0.065	0.007	0.032	0.032	−0.012	−0.030	−0.030	0.000	0.000	0.000	0.000
0.199	−0.120	0.069	0.069	0.029	−0.023	−0.023	0.000	0.000	0.000	0.000
−0.225	0.234	0.087	0.087	−0.112	−0.153	−0.153	0.000	0.000	0.000	0.000
−0.031	0.274	−0.298	−0.298	−0.283	0.301	0.301	0.000	0.000	0.000	0.000
−0.059	−0.304	0.322	−0.284	0.280	0.296	−0.298	−0.065	−0.001	0.004	−0.001
−0.059	−0.304	−0.284	0.322	0.280	−0.298	0.296	0.065	0.001	−0.004	0.001
−0.378	−0.028	0.041	0.041	−0.015	−0.020	−0.020	0.000	0.000	0.000	0.000
0.017	0.002	−0.001	−0.001	−0.003	0.001	0.001	0.000	0.000	0.000	0.000
0.009	0.017	−0.005	−0.005	−0.005	−0.001	−0.001	0.000	0.000	0.000	0.000
−0.415	0.074	−0.015	−0.015	−0.016	−0.015	−0.015	0.000	0.000	0.000	0.000
0.793	−0.046	−0.026	−0.026	0.031	0.035	0.035	0.000	0.000	0.000	0.000
	1.087	−0.118	−0.118	−0.421	−0.231	−0.231	0.000	0.000	0.000	0.000
		0.922	0.010	−0.211	−0.239	−0.379	−0.097	−0.001	−0.015	−0.004
			0.922	−0.211	−0.379	−0.239	0.097	0.001	0.015	0.004
				1.284	−0.202	−0.202	0.000	0.000	0.000	0.000
					1.275	−0.211	−0.018	0.000	0.000	−0.002
						1.275	0.018	0.000	0.000	0.002
							0.431	0.003	−0.010	0.010
								0.018	0.000	0.003
									0.006	−0.001
										0.014

ϵ	β_1	β_2	β_3	α_1	α_2	α_3	ω	π	τ_1	τ_2
0.186	0.147	0.004	0.004	−0.110	−0.028	−0.028	0.000	0.000	0.000	0.000
0.176	−0.032	−0.045	−0.045	0.042	0.041	0.041	0.000	0.000	0.000	0.000
0.032	0.070	0.012	0.012	−0.063	−0.018	−0.018	0.000	0.000	0.000	0.000
0.193	−0.125	0.075	0.075	0.034	−0.027	−0.027	0.000	0.000	0.000	0.000
−0.252	0.207	0.118	0.118	−0.112	−0.172	−0.172	0.000	0.000	0.000	0.000
−0.014	0.247	−0.294	−0.294	−0.276	0.301	0.301	0.000	0.000	0.000	0.000
−0.068	−0.328	0.354	−0.283	0.318	0.255	−0.294	−0.086	−0.001	−0.021	−0.016
−0.068	−0.328	−0.283	0.354	0.318	−0.294	0.255	0.086	0.001	0.021	0.016
−0.349	−0.025	0.025	0.025	−0.010	−0.008	−0.008	0.000	0.000	0.000	0.000
−0.015	0.005	0.001	0.001	−0.011	0.002	0.002	0.000	0.000	0.000	0.000
−0.043	0.016	0.013	0.013	−0.022	−0.010	−0.010	0.000	0.000	0.000	0.000
−0.436	0.064	0.011	0.011	−0.028	−0.030	−0.030	0.000	0.000	0.000	0.000
0.785	−0.039	−0.036	−0.036	0.038	0.038	0.038	0.000	0.000	0.000	0.000
	1.049	−0.129	−0.129	−0.409	−0.217	−0.217	0.000	0.000	0.000	0.000
		0.962	0.011	−0.215	−0.253	−0.384	−0.089	0.001	−0.017	0.006
			0.962	−0.215	−0.384	−0.253	0.089	−0.001	0.017	−0.006
				1.306	−0.203	−0.203	0.000	0.000	0.000	0.000
					1.270	−0.208	−0.013	0.000	0.005	0.004
						1.270	0.013	0.000	−0.005	−0.004
							0.411	−0.006	−0.011	−0.022
								0.024	0.000	0.002
									0.007	−0.001
										0.008

Table 7

Observed and calculated frequencies (cm^{-1}) and potential energy distribution (P.E.D.) calculated with the MP2/6-31G* basis set for the cis and trans conformers of trifluoroacetyl isocyanate

Species	Vib. no.	Fundamental	Cis				Trans			
			Ab initio	IR int.[a]	Obs.[b]	P.E.D.	Ab initio	IR int.[a]	Obs.[b]	P.E.D.
A′	ν_1	NCO antisymmetric stretch	2361	1002.1	2235	$99S_1$	2373	985.2		$99S_1$
	ν_2	CO stretch	1811	184.6	1781	$91S_2$	1827	385.1	1796	$91S_2$
	ν_3	NCO symmetric stretch	1502	235.9	1463	$43S_3, 32S_7, 12S_4$	1498	130.0	1443	$52S_3, 33S_7$
	ν_4	CC stretch	1360	159.6	1309	$23S_4, 22S_3, 18S_6, 14S_8, 13S_5$	1356	150.0		$19S_4, 27S_5, 17S_6, 13S_3, 12S_8$
	ν_5	CF_3 antisymmetric stretch	1296	210.4	1242	$67S_5$	1295	126.1		$54S_5, 11S_4$
	ν_6	CF_3 symmetric stretch	1051	340.4	1025	$25S_6, 26S_7, 21S_3, 15S_{11}$	1059	247		$23S_6, 25S_7, 23S_{11}, 16S_3$
	ν_7	CN stretch	821	27.1	808	$21S_7, 25S_6, 11S_4, 11S_9$	779	15.2	776	$10S_7, 47S_6, 16S_4, 19S_8$
	ν_8	CF_3 symmetric deformation	729	91.6	737	$33S_8, 24S_6, 18S_{11}, 14S_9$	625	21.6	626	$20S_8, 21S_{13}, 11S_{11}$
	ν_9	NCO bend	598	12.4	601	$28S_9, 22S_{10}, 14S_{13}, 12S_{12}, 10S_5$	656	7.4		$61S_9$
	ν_{10}	CF_3 antisymmetric deformation	564	0.4	571	$26S_{10}, 35S_9, 13S_7, 10S_{11}$	567	9.0		$35S_{10}, 18S_9, 14S_7$
	ν_{11}	CC(O)N bend	420	1.6	420	$23S_{11}, 33S_{10}, 12S_4, 11S_{12}, 10S_8$	383	0.2	380	$31S_{11}, 36S_4, 25S_8$
	ν_{12}	CF_3 rock	359	1.6	355	$24S_{12}, 24S_4, 16S_8, 11S_{11}$	256	8.3		$53S_{12}, 24S_{13}, 13S_{14}$
	ν_{13}	CCN deformation	230	0.6	232	$36S_{13}, 35S_{12}, 15S_{14}$	422	5.9		$20S_{13}, 43S_{10}, 14S_{12}$
	ν_{14}	CNC bend	100	0.8	90	$72S_{14}, 16S_{13}$	98	0.05		$73S_{14}, 17S_{13}$
A″	ν_{15}	CF_3 antisymmetric stretch	1252	262.7	1195	$84S_{15}, 10S_{18}$	1228	256.8		$84S_{15}$
	ν_{16}	CC(O)N bend	766	12.9	752	$63S_{16}, 24S_{19}$	752	9.0		$60S_{16}, 25S_{19}$
	ν_{17}	NCO bend	607	25.6	611	$92S_{17}$	584	19.6		$93S_{17}$
	ν_{18}	CF_3 antisymmetric deformation	513	5.8	517	$85S_{18}$	508	9.4		$83S_{18}$
	ν_{19}	CF_3 rock	251	3.7	254	$69S_{19}, 18S_{16}$	250	5.4		$71S_{19}, 21S_{16}$
	ν_{20}	NCO torsion	76	0.3	75	$80S_{20}$	95	0.8	93	$63S_{20}, 31S_{21}$
	ν_{21}	CF_3 torsion	41	0.6		$91S_{21}$	26	0.2		$60S_{21}, 34S_{20}$

[a] Calculated with the MP2/6-31G* basis set in km mol^{-1}.

[b] Frequencies are taken from the infrared or Raman spectra of the gas.

Table 8

Observed and calculated frequencies (cm^{-1}) and potential energy distribution (P.E.D.) calculated using the RHF/6-31G* basis set for the cis and trans conformers of trifluoroacetyl isocyanate

Species	Vib. no.	Fundamental	Cis						Trans					
			Ab initio	Fixed scaled[a]	IR int.[b]	Raman act.[c]	Obs.[d]	P.E.D.	Ab initio	Fixed scaled[a]	IR int.[b]	Raman act.[c]	Obs.[d]	P.E.D.
A′	ν_1	NCO antisymmetric stretch	2481	2354	1577.4	4.3	2235	$98S_1$	2504	2375	1715.6	3.1		$97S_1$
	ν_2	CO stretch	2054	1945	332.5	17.9	1781	$92S_2$	2079	1969	725.7	39.5	1796	$92S_2$
	ν_3	NCO symmetric stretch	1624	1533	330.2	9.0	1463	$48S_3, 32S_7$	1668	1580	183.0	15.1	1443	$61S_3, 31S_7$
	ν_4	CC stretch	1480	1387	205.7	3.6	1309	$23S_4, 19S_6, 19S_5, 18S_3, 11S_8$	1492	1396	147.7	3.1		$18S_4, 38S_5, 16S_6$
	ν_5	CF_3 antisymmetric stretch	1427	1341	269.6	1.0	1242	$66S_5$	1425	1337	169.7	2.2		$47S_5, 16S_4, 12S_6$
	ν_6	CF_3 symmetric stretch	1148	1075	401.1	2.7	1025	$28S_6, 31S_7, 18S_3, 12S_{11}$	1144	1065	348.7	1.0		$27S_6, 28S_7, 21S_{11}, 14S_3$
	ν_7	CN stretch	918	849	66.2	6.7	808	$19S_7, 23S_6, 14S_8, 13S_4$	850	795	27.3	6.3	776	$12S_7, 41S_6, 20S_8, 17S_4$
	ν_8	CF_3 symmetric deformation	812	739	102.5	1.5	737	$34S_8, 21S_6, 18S_{11}, 17S_9$	682	619	25.2	3.1	626	$23S_8, 22S_{13}, 14S_{11}$
	ν_9	NCO bend	663	597	26.1	0.7	601	$41S_9, 14S_{13}, 11S_8, 10S_{10}$	738	661	27.2	0.5		$75S_9$
	ν_{10}	CF_3 antisymmetric deformation	624	566	0.7	1.3	571	$40S_{10}, 16S_9, 11S_5, 10S_7, 10S_{11}$	623	568	10.7	2.3		$41S_{10}, 13S_7, 11S_5, 10S_{11}$
	ν_{11}	CC(O)N bend	460	415	2.2	0.7	420	$24S_{11}, 33S_{10}, 13S_4, 11S_8, 10S_{12}$	416	380	0.4	2.3	380	$25S_{11}, 31S_4, 25S_8, 10S_{13}$
	ν_{12}	CF_3 rock	386	351	2.0	1.8	355	$27S_{12}, 21S_4, 16S_8, 10S_{10}, 10S_{11}$	460	414	8.9	0.6		$14S_{12}, 42S_{10}, 16S_{13}, 15S_{11}$
	ν_{13}	CCN deformation	248	222	0.6	0.8	232	$38S_{12}, 34S_{12}, 15S_{14}$	271	243	11.8	0.2		$29S_{13}, 52S_{12}, 12S_{14}$
	ν_{14}	CNC bend	107	96	0.9	2.0	90	$73S_{14}, 16S_{13}$	94	84	0.3	1.1		$81S_{14}, 12S_{13}$
A″	ν_{15}	CF_3 antisymmetric stretch	1385	1304	304.2	1.8	1195	$88S_{15}$	1361	1280	303.3	1.6		$88S_{15}$
	ν_{16}	CC(O)N bend	854	768	33.6	0.1	752	$66S_{16}, 23S_{19}$	839	754	21.1	0.6		$64S_{16}, 25S_{19}$
	ν_{17}	NCO bend	707	637	57.7	0.3	611	$91S_{17}$	687	617	58.0	0.4		$95S_{17}$
	ν_{18}	CF_3 antisymmetric deformation	564	507	9.6	0.7	517	$86S_{18}$	559	502	14.0	1.0		$86S_{18}$
	ν_{19}	CF_3 rock	279	252	5.4	0.1	254	$69S_{19}, 16S_{16}$	274	246	8.2	1.0		$73S_{19}, 20S_{16}$
	ν_{20}	NCO torsion	80	79	0.6	1.9	75	$75S_{20}$	93	93	0.9	0.04	93	$61S_{20}, 34S_{21}$
	ν_{21}	CF_3 torsion	47	47	0.8	0.6		$88S_{21}, 11S_{20}$	21	21	0.2	0.9		$58S_{21}, 37S_{20}$

[a] Scaled ab initio calculations with factors of 0.9 for stretches and 0.8 for bends, and 1.0 for torsion using the RHF/6-31G* basis set.

[b] Calculated infrared intensities in km mol^{-1}.

[c] Calculated Raman activities in Å^4 amu^{-1}.

[d] Frequencies are taken from the infrared and/or Raman spectrum of the gas.

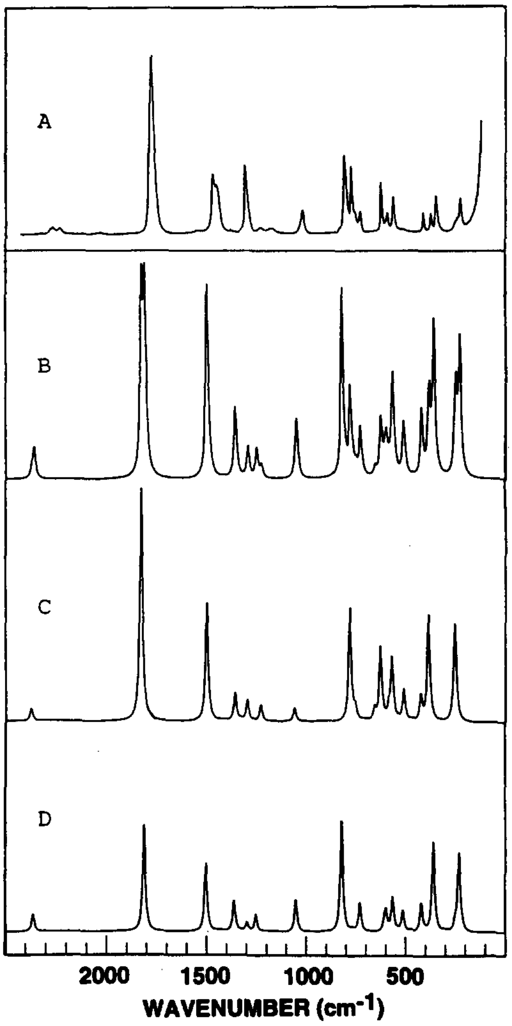

Fig. 9. Raman spectra of trifluoroacetyl isocyanate: (A) experimental Raman spectrum of the liquid; (B) calculated spectrum of the mixture of both conformers; (C) calculated spectrum of the trans conformer; (D) calculated spectrum of the cis conformer.

trans pure conformers are shown in Figs. 9(D) and 9(C), respectively. In Fig. 9(B), the mixture of the two conformers with an assumed ΔH of 163 cm^{-1} is shown. This spectrum should be compared to the experimental Raman spectrum of the liquid (Fig. 9(A)). In comparison, the calculated spectrum is remarkably similar to the experimental spectrum and provides support for the assignment of the observed bands.

Infrared intensities were also calculated based on the dipole moment derivatives with respect to the Cartesian coordinates. The derivatives were taken from the ab initio calculations transformed to normal coordinates by

$$\left(\frac{\partial \mu_u}{\partial Q_i}\right) = \sum_j \left(\frac{\partial \mu_u}{\partial X_j}\right) \boldsymbol{L}_{ji}$$

where the Q_i is the ith normal coordinate, X_j is the jth Cartesian displacement coordinate, and $\boldsymbol{L}_{ji}$ is the transformation matrix between the Cartesian displacement coordinates and normal coordinates. The infrared intensities were then calculated by

$$I_i = \frac{N\pi}{3C^2}\left[\left(\frac{\partial \mu_x}{\partial Q_i}\right)^2 + \left(\frac{\partial \mu_y}{\partial Q_i}\right)^2 + \left(\frac{\partial \mu_z}{\partial Q_i}\right)^2\right]$$

The predicted infrared spectra of the pure cis and trans conformers are shown in Figs. 10(D) and 10(C), respectively, with the mixture of the two conformers shown in Fig. 10(B). The calculated spectrum is in reasonably good agreement with the experimental spectrum of the gas (Fig. 10(A)) and demonstrates the utility of the calculated infrared intensities for analytical purposes.

6. Asymmetric potential function

The torsional dihedral angular dependence of the internal rotation constant $F(\phi)$ can be represented as a Fourier series:

$$F(\phi) = F_0 + \sum_{i=1}^{6} F_i \cos i\phi$$

The relaxation of the structural parameters $\boldsymbol{B}(\phi)$ during the internal rotation can be incorporated into the above equation by assuming them to be small periodic functions of the torsional angle of the general type:

$$B(\phi) = a + b \cos \phi + c \sin \phi$$

The structural parameters obtained from the optimized geometries for both the cis and trans conformers utilizing the MP2/6-31G* basis set were used to determine $B(\phi)$.

The torsional potential is also represented as a

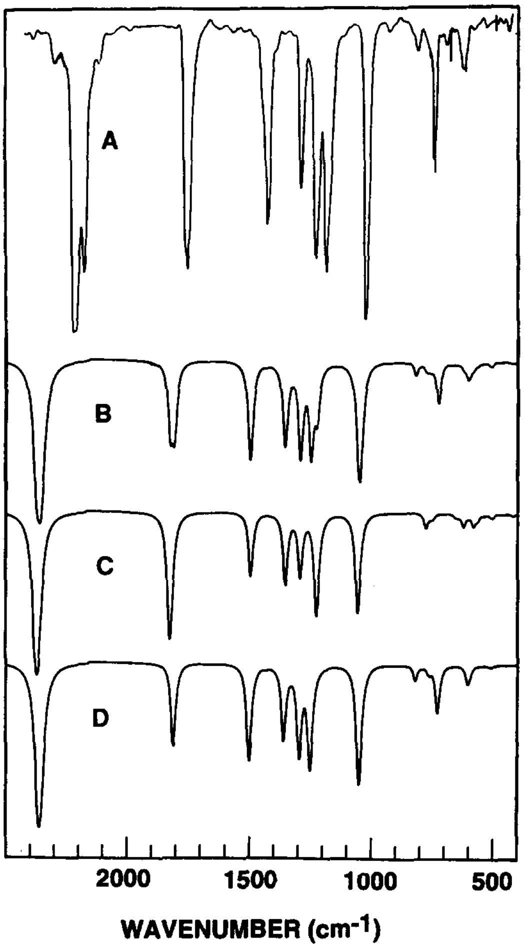

Fig. 10. Infrared spectrum of trifluoroacetyl isocyanate: (A) experimental infrared spectrum of the gas; (B) calculated spectrum of the mixture of both conformers; (C) calculated spectrum of the trans conformer; (D) calculated spectrum of the cis conformer.

Fourier cosine series in the internal dihedral torsional angle (ϕ):

$$V(\phi) = \sum_{i=1}^{6} (V_i/2)(1 - \cos i\phi)$$

The computer program which was employed was developed in our laboratory [25].

Previous calculations on the potential functions for many molecules with a cis–trans equilibrium indicate that only the V_1, V_2, and V_3 coefficients are likely to be significant. Thus, these potential coefficients were used to fit the experimental data. The fundamental torsional transition for the cis conformer, the observed fundamental torsional transition for the trans conformer and the experimental enthalpy difference ($163 \pm 12\,\text{cm}^{-1}$) from the temperature study of the infrared spectrum of the sample dissolved in liquified krypton were used to calculate initial values of 356, 1865, and $-203\,\text{cm}^{-1}$ for the potential constants, V_1, V_2, and V_3, respectively. Since there was only one observable torsional transition for each of the conformers, the enthalpy difference was varied by $\pm 12\,\text{cm}^{-1}$ and the calculation was repeated. Therefore, the final values for the potential coefficients with the uncertainties are $V_1 = 356 \pm 14$, $V_2 = 1865 \pm 60$ and $V_3 = -203 \pm 6\,\text{cm}^{-1}$ with cis to trans and trans to cis barriers of $1971\,\text{cm}^{-1}$ ($5.6\,\text{kcal mol}^{-1}$) and $1811\,\text{cm}^{-1}$ ($5.2\,\text{kcal mol}^{-1}$), respectively. The resulting values for the potential constants are listed in Table 9 and the potential function is shown in Fig. 11.

7. Discussion

It has been determined that the cis conformer is the more stable rotamer in the fluid phases and the only conformer present in the solid. The cis conformer is predominant in the gas, but there is evidence that a second conformer is present. It is clear from the temperature study of the sample

Table 9
Potential function coefficients (cm^{-1}) for the asymmetric torsion of trifluoroacetyl isocyanate and barriers to interconversion (cm^{-1})

Coefficient	Value[a]	Ab initio MP2/6-31G*
V_1	356 ± 14	222
V_2	1865 ± 60	1009
V_3	−203 ± 6	126
ΔH (cm^{-1})	160 ± 16	349
Torsional frequency (cis)	74.0	79
Torsional frequency (trans)	93.0	93
Cis to trans barrier	1971	1185
Trans to cis barrier	1811	836

[a] Calculated using $F_0 = 0.86979$, $F_1 = -0.03234$, $F_2 = 0.09152$, $F_3 = -0.00172$, $F_4 = 0.00507$, $F_5 = -0.00007$, $F_6 = 0.00028$ (cm^{-1}) and the assignments of the torsional transitions listed in Table 1.

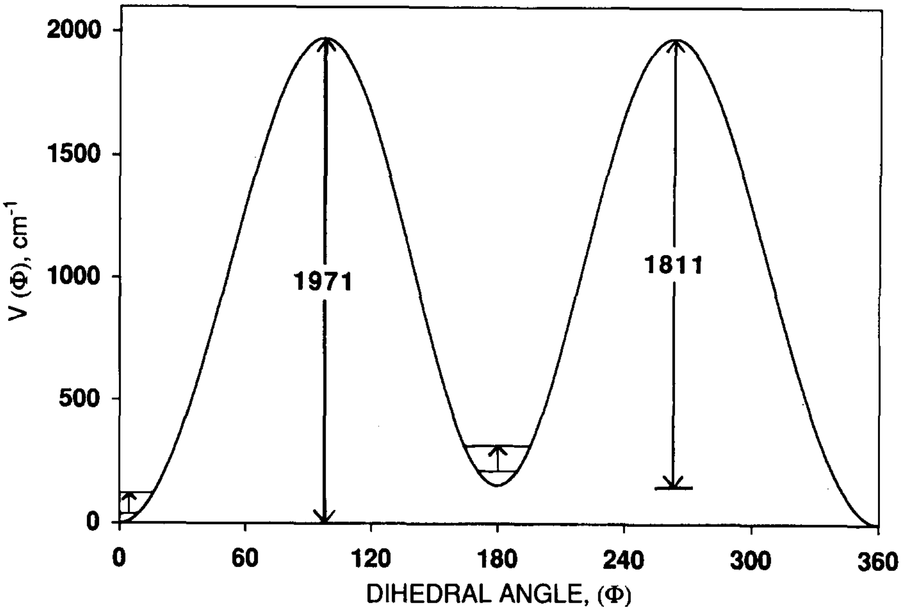

Fig. 11. Potential function for the interconversion of the conformers of trifluoroacetyl isocyanate.

dissolved in liquified krypton (Table 2) that the band at 1785 cm^{-1}, which is assigned to the CO stretch of the cis conformer, increases in intensity as the temperature is decreased and thus is the stable rotamer in the gas phase. Similarly, from the temperature study of the Raman spectrum of the liquid, the bands at 776, 626, and 380 cm^{-1}, which are assigned to fundamentals of the trans conformer, increase in intensity as the temperature is increased, showing that the trans conformer is also less stable than the cis rotamer in the liquid phase.

It is interesting to compare the conformational stability of $CF_3C(O)NCO$ with $CH_3C(O)NCO$ [1] and FC(O)NCO [9]. In all three molecules, the cis conformer was determined to be the more stable form in the vapor site. However, for $CH_3C(O)NCO$ and FC(O)NCO, it was experimentally determined that the trans conformer is the stable conformer that remains in the solid phase, which is in contrast to what was found for $CF_3C(O)NCO$, where it has been determined that the cis conformer is the stable rotamer in the solid state. However, for $CH_3C(O)NCO$ [1], the trans conformer was the more stable rotamer in the liquid state, whereas for the $CF_3C(O)NCO$ molecule, the cis conformer was the more stable form in the liquid. For ClC(O)NCO it was determined experimentally [4] that the trans conformer is the stable form in the gas, liquid, and solid phases. Therefore, the molecule with the chlorine atom is the exception for conformational stability in the gas phase for this series of molecules.

There is extensive mixing among the normal modes especially for the ν_4 and ν_6 through ν_{13} fundamentals of the cis conformer as determined from the ab initio calculations with the MP2/6-31G* basis set. The band observed at 808 cm^{-1}, which is assigned to the C–N stretch, has 21% contribution from the C–N stretch and 25% from the CF_3 symmetric stretch. There is extensive mixing between the A′ NCO bend and A′ CF_3 antisymmetric deformation. The band at 601 cm^{-1}, which is assigned to the NCO bend has 28 and 22% contribution from the NCO bend and CF_3 antisymmetric deformation, respectively. Similarly, the band at 571 cm^{-1} assigned to the CF_3 antisymmetric deformation has 26% contribution from the CF_3 antisymmetric deformation and 35% contribution from the NCO bend. The observed band at 420 cm^{-1} which has been assigned to the CC(O)N bend actually has more contribution from the CF_3 antisymmetric deformation. There is also extensive mixing among the fundamentals of the trans conformer, especially for the C–N stretch and CF_3 symmetric deformation. The observed band at $776\,cm^{-1}$ assigned to the CN stretch has more contribution from the CF_3 symmetric stretch, whereas the band at $626\,cm^{-1}$ assigned to the CF_3 symmetric deformation has an equal contribution from the CCN deformation. Therefore, the simple descriptions given to each of the bands listed in Tables 7 and 8 are more for "bookkeeping" purposes than actual descriptions of the molecular motions.

The force constants from the ab initio calculations for the two rotamers of $CF_3C(O)NCO$ are fairly similar with a few notable exceptions. The CNC bend, NCO out-of-plane bend, and CF_3 torsion have values of 0.377, 0.018, and $0.014\,mdyn\,Å^{-1}$, respectively, for the cis conformer which are significantly different from the values of 0.485, 0.024, and $0.008\,mdyn\,Å^{-1}$ for the corresponding force constants for the trans form. The force constants for $CF_3C(O)NCO$ are comparable to those obtained for the portion of the molecule which is identical with the acetyl isocyanate molecule. Significant exceptions are the NCO in-plane and out-of-plane bends and the CC(O)N bend of the cis conformer where the values are 0.896, 0.014, and $0.568\,mdyn\,Å^{-1}$, respectively, for $CH_3C(O)NCO$ [1] which should be contrasted to the values of 0.695, 0.018, and $0.431\,mdyn\,Å^{-1}$ for the corresponding force constants, respectively, for $CF_3C(O)NCO$. The notable exceptions of the trans conformer are the CNC bend, CC(O)N bend, NCO out-of-plane bend, and the NCO torsion which have values of 0.279, 0.564, 0.015, and $0.004\,mdyn\,Å^{-1}$ for $CH_3C(O)NCO$ compared with those of 0.485, 0.411, 0.024, and $0.008\,mdyn\,Å^{-1}$ for $CF_3C(O)NCO$.

The calculated infrared spectrum of the mixture of the two conformers (Fig. 10(B)) is comparable to the experimental spectrum of the gas. However, the region from 2500 to $1600\,cm^{-1}$ in the calculated spectrum differs from the experimental spectrum. There are two bands in the NCO antisymmetric stretching region in the experimental spectrum as opposed to only one band in the calculated spectrum. There are two bands in the CO stretching region in the calculated spectrum whereas only one band appears in this region in the experimental infrared spectrum of the gas. When comparing the relative intensities of the bands in the region from 1400 to $400\,cm^{-1}$, the experimental and calculated spectra are remarkably similar.

The calculated Raman spectrum of the mixture of the two conformers (Fig. 9(B)) is also comparable to the experimental spectrum of the liquid. As in the experimental infrared spectrum of the gas, there are two bands present in the experimental Raman spectrum of the liquid in the NCO antisymmetric stretching region, where one band is due to two fundamentals. The NCO antisymmetric stretch is predicted about $100\,cm^{-1}$ higher while the CO and NCO symmetric stretches are predicted only about 30 to $40\,cm^{-1}$ higher in the calculated spectrum. The region from 1000 to $200\,cm^{-1}$ is similar between the calculated and experimental data except for the relative intensity of the CF_3 symmetric deformation which is less than the relative intensity for this fundamental in the experimental spectrum. The low-frequency fundamentals (CNC bend and NCO and CF_3 torsions) were omitted from the calculated spectra because of their large intensities which, if included, would render all other bands unobservable with the relative scale which was used.

The potential function for the NCO asymmetric torsion of $CF_3C(O)NCO$ has been estimated from the observed torsional transitions and a ΔH value of $163 \pm 12\,cm^{-1}$. Only one torsional transition was observed for each conformer, where the transition at $75\,cm^{-1}$ has been assigned to the asymmetric torsion of the cis conformer, and the transition for this mode of the trans conformer has been assigned to the band at $93\,cm^{-1}$. It should be noted that the CNC bend is predicted in this region at about $100\,cm^{-1}$. The NCO torsion of the cis and trans conformers of $CF_3C(O)NCO$ were observed in the same region of the infrared spectrum of the gas as those observed for some similar molecules. For acetyl isocyanate [1], the torsional mode of the cis conformer was observed at $79\,cm^{-1}$ in the infrared spectrum of the gas with two excited states falling to lower frequency. However, the asymmetric torsion of the less stable trans conformer was not observed. The NCO torsion of the cis conformer of fluorocarbonyl isocyanate [9] was observed at 82 cm^{-1} with six excited states falling to lower frequencies, whereas this mode of the less stable trans conformer was tentatively assigned to the weaker band at 88 cm^{-1}. Similarly, this mode of the more stable trans conformer of ClC(O)NCO [4] was observed at 83 cm^{-1} in the infrared spectrum of the gas with two excited states falling to lower frequencies, while the asymmetric torsion of the cis conformer was not observed.

Because there was only one observable torsional transition for the NCO torsion of each conformer, the uncertainties of the potential coefficients were estimated by varying the experimental ΔH value of 163 cm^{-1} by ± 12 cm^{-1}. The resulting potential coefficients and their uncertainties are listed in Table 9. The potential function obtained from ab initio calculations with the MP2/6-31G* basis set is considerably different to that determined from the experimental data. The ΔH value obtained with the MP2/6-31G* basis set is twice as large as the experimental ΔH. There have been several barriers reported for the NCO asymmetric torsion. The cis to trans and trans to cis barriers for CF_3CONCO are larger than those reported for acetyl isocyanate [1] and chlorocarbonyl isocyanate [4], as well as those for fluorocarbonyl isocyanate [9], which were the largest of those previously reported with cis to trans and trans to cis barriers of 1116 and 991 cm^{-1}, respectively. The significant increases in the barriers for the trifluoroacetyl isocyanate molecule is probably due to the increase in steric hindrance caused by the perfluoromethyl group.

There are only very small differences (0.005 Å) in the bond distances between the two rotamers, but some of the angles are significantly different. For example, the $\measuredangle C_1{-}N{=}C$ increases by 4.1° and the $\measuredangle C{-}C{-}N$ opens by 3.6° on going from the cis to the trans conformation, which again indicates strong steric interaction of the perfluoromethyl group with the isocyanate group. The other angles differ by less than 1° between the two conformers. There are significant differences in the bond distances calculated with the RHF/6-31G* basis set and those with electron correlation, MP2/6-31G*. For the carbonyl bonds, the predicted distances with the MP2/6-31G* basis set will be too long by nearly the amount that the RHF/6-31G* basis set predicts them to be too short [26]. In fact, the RHF/3-21G* predicts these bond distances better.

It is interesting to compare the predicted structural parameters for trifluoroacetyl isocyanate utilizing the MP2/6-31G* basis set with those predicted [2] for acetyl isocyanate utilizing the same basis set. The predicted differences are relatively small, with the $r(C_3{=}O_4)$ and $r(C_1{=}O_5)$ calculated to be shorter by 0.005 and 0.004 Å, respectively, for the perfluoro compound, whereas the $r(N{=}C_3)$ distance is predicted to be longer by 0.003 Å. Therefore, one should be able to take these parameters for the acetyl isocyanate molecule, which were determined by a joint analysis of the electron diffraction and microwave data, and make these adjustments to give realistic distances for these three parameters. The $r(C_1{-}N)$ distance is predicted to be 0.025 Å shorter for the trifluoroacetyl isocyanate molecules, whereas the $r(C_1{-}C_6)$ distance is predicted to be 0.028 Å longer than the corresponding distances for acetyl isocyanate. The only other parameter with a significant difference between these two molecules is the $N{-}C_1{=}O$ angle which is predicted to be 2.4° larger for the perfluoro molecule. These differences reflect the effect of the fluorine atoms on these latter three parameters. Thus, one should be able to take the parameters obtained from the ab initio calculations with the MP2/6-31G* basis set and utilize the indicated adjustments and predict structural parameters which should be accurate to about 0.010 Å for distances and about 1.0° for angles for trifluoroacetyl isocyanate.

References

[1] J.R. Durig, G.A. Guirgis, K.A. Krutules and J.F. Sullivan, J. Raman Spectrosc., 24 (1993) 259.

[2] B.M. Landsberg and K. Iqbal, J. Chem. Soc., Faraday Trans. 2, 76 (1980) 1208.

[3] H.G. Mack, H. Oberhammer and C.O. Della Vedova, J. Mol. Struct., 265 (1992) 359.

[4] J.F. Sullivan, S.K. Nandy, M.J. Lee and J.R. Durig, J. Raman Spectrosc., 23 (1992) 51.

[5] H.G. Mack, H. Oberhammer and C.O. Della Vedova, J. Mol. Struct., 200 (1989) 277.

[6] M.T. Nguyen, M.R. Hajnal and L.G. Vanquickenborne, J. Mol. Struct., 231 (1991) 185.

[7] H.G. Mack and H. Oberhammer, J. Mol. Struct. (Theochem), 258 (1992) 197.
[8] V. Jonas and G. Frenking, Chem. Phys. Lett., 177 (1991) 175.
[9] J.R. Durig, G.A. Guirgis, K.A. Krutules, H.V. Phan and H.D. Stidham. J. Raman Spectrosc., 25 (1994) 221.
[10] H.G. Mack, C.O. Della Vedova and H. Willner, J. Mol. Struct., 291 (1993) 197.
[11] J.R. Durig, M.R. Jalilian, J.F. Sullivan and J.B. Turner, J. Raman Spectrosc., 11 (1981) 459.
[12] J.R. Durig, K.J. Kanes and J.F. Sullivan, J. Mol. Struct., 99 (1983) 61.
[13] S. Cradock, J.R. Durig and J.F. Sullivan, J. Mol. Struct., 131 (1985) 121.
[14] S. Cradock, C.M. Huntley and J.R. Durig, J. Mol. Struct., 127 (1985) 319.
[15] S. Cradock, J.F. Sullivan and J.R. Durig, J. Mol. Struct., 140 (1986) 199.
[16] J.F. Sullivan, D.T. Durig, J.R. Durig and S. Cradock, J. Phys. Chem., 91 (1987) 1770.
[17] J.R. Durig and G.M. Attia, Spectrochim. Acta, Part A, 44 (1988) 517.
[18] J.R. Durig, R.J. Berry and C.J. Wurrey, J. Am. Chem. Soc., 110 (1988) 718.
[19] J.F. Sullivan, H.L. Heusel, W.M. Zunic, J.R. Durig and S. Cradock, Spectrochim. Acta, Part A, 50 (1994) 435.
[20] F.A. Miller and B.M. Harney, Appl. Spectrosc., 24 (1970) 291.
[21] M.J. Frisch, M. Head-Gordon, G.W. Trucks, J.B. Foresman, H.B. Schlegel, K. Raghavachari, M.A. Robb, J.S. Binkley, C. Gonzalez, D.J. DeFrees, D.J. Fox, R.A. Whiteside, R. Seeger, C.F. Melius, J. Baker, R.L. Martin, L.R. Kahn, J.J.P. Stewart, S. Topiol and J.A. Pople, GAUSSIAN 90, Gaussian, Inc., Pittsburgh, PA, 1990.
[22] P. Pulay, Mol. Phys., 17 (1969) 197.
[23] J.H. Schachtschneider, Vibrational Analysis of Polyatomic Molecules, Parts V and VI, Technical Report Nos. 231 and 57, Shell Development Co., Houston, TX, 1964 and 1965.
[24] G.W. Chantry, in A. Anderson (Ed.), The Raman Effect, Vol. 1, Marcel Dekker, New York, NY, 1971, Chapter 2.
[25] P. Groner, R.D. Johnson and J.R. Durig, J. Mol. Struct., 142 (1986) 363.
[26] J.R. Durig, T.J. Geyer, Y.H. Kim, V.F. Kalasinsky and J.K. McDonald, J. Mol. Struct., 244 (1991) 103.